Contribution from the Department of Chemistry,
McMaster University, Hamilton, Ontario, Canada L8S 4M1

Molecular Orbital Investigation of the Structure of Some Polyatomic Cations and Anions of the Main-Group Elements

ROBERT C. BURNS, RONALD J. GILLESPIE,* JOHN A. BARNES, and MICHAEL J. McGLINCHEY*

Received November 5, 1980

The extended-Hückel molecular orbital approach and the Jahn-Teller theorem have been applied to a consideration of the structures of the Te_4^{2+}, Bi_4^{2-}, Sn_5^{2-}, Bi_5^{3+}, Pb_5^{2-}, Te_6^{4+}, P_6^{4-}, Te_6^{2+}, P_7^{3-}, Sb_7^{3-}, S_8^{2+}, Sn_9^{4-}, and P_{11}^{3-} ions. The stability and diamagnetism of these species have been accounted for in terms of a closed-shell molecular orbital configuration for each of the observed geometries. Alternative geometries were also investigated for four- through six-, eight-, and nine-membered species and in almost every case shown either to be unfavorable in terms of total energy or to be electronically (Jahn-Teller) unstable, undergoing nuclear rearrangement to give the observed structure. Application of the second-order Jahn-Teller arguments were, however, not always conclusive because of the inability of the extended-Hückel procedure to accurately calculate molecular orbital energy levels for these heavy atom systems, particularly the important HOMO-LUMO energy gap. Reliable results were obtained for those ions in which symmetry constraints allowed a realistic ordering of molecular orbitals, and for which a reasonable estimate of the energy difference between the HOMO and LUMO could be made, such as geometries involving π manifolds. In cases where less definitive results were obtained, resort to more rigorous calculations such as a CNDO study always enabled conclusions to be drawn from symmetry considerations and led to a reasonable interpretation of the particular system.

Introduction

Over the past few years, a considerable number of homo- and heteropolyatomic cations and anions of the main-group elements have been characterized. These species exhibit a wide variety of structural forms including chains, rings, cages, and clusters.[1,2] However, while many are amenable to a localized two-electron two-center bonding description, others can only be represented by a multitude of canonical forms and require charge dispersal over the entire system. Still others adopt structures akin to those of the boranes and carboranes. The application of molecular orbital (MO) theory to all of these species is, therefore, of considerable interest because of the diversity of structural types and lack of a comprehensive bonding picture afforded by a valence-bond treatment.

The first application of LCAO-MO methods to polyatomic cluster species of this type was reported for the Bi_9^{5+} cation by Corbett and Rundle.[3] With use of an idealized tricapped trigonal-prismatic geometry and a basis set consisting only of 6p atomic orbitals and by including all important overlaps, the stability and observed diamagnetism of Bi_9^{5+} was accounted for in terms of a closed-shell configuration with the 22 p electrons in 11 bonding MO's. Subsequent MO studies by Corbett[4] on Bi_5^{3+} and Bi_8^{2+} suggested that these species had trigonal-bipyramidal and square-antiprismatic structures, respectively. Indeed, the trigonal-bipyramidal geometry for Bi_5^{3+} was recently confirmed by a vibrational spectroscopic study,[5] and this same paper also contained a preliminary EHMO treatment of the Bi_5^{3+} species. Other studies have been reported on the square-planar S_4^{2+}, Se_4^{2+}, and Te_4^{2+} cations using MO procedures of various levels of sophistication such as the simple Hückel[6] and EHMO[7] approaches, a semiempirical INDO-type ASMO-SCF method,[8] an ab initio pseudopotential SCF procedure,[9] and the SCF-Xα-SW approach.[10] The INDO method has also been applied by the same authors to a study of S_8^{2+} and Se_8^{2+}.[11] In their extensive treatment of the structural changes on oxidation and reduction of the sulfur species S_3, S_4, S_6, and S_8, Salahub et al.[10] also examined S_8^{2+} and S_8^{4+} (the "dimer" of S_4^{2+} and an analogue of S_4N_4) and the hypothetical S_4^{4+} and S_6^{2+} cations using the SCF-Xα-SW procedure.

Table I. Valence-State Orbital Ionization Energies for P, S, Sn, Sb, Te, Pb, and Bi[a]

element	H_{ii} (*n*s)	H_{ii} (*n*p)	element	H_{ii} (*n*s)	H_{ii} (*n*p)
P[b]	-18.67	-11.89	Te[b]	-17.63	-9.79
S[c]	-23.06	-10.36	Pb[b]		-9.18
Sn[d]	-16.16	-8.32	Bi[b]		-9.24
Sb[e]	-16.70	-9.00			

[a] Units are in eV. [b] Reference 15. [c] Reference 16. [d] Reference 17. [e] Extrapolated value based on data given in ref 15.

The simplicity, utility, and economy of extended-Hückel MO (EHMO) calculations over a wide range of geometries has been well-proven in studies of the borane and related systems, as well as conventionally coordinated species. Furthermore, the EHMO approach, in conjunction with the Jahn-Teller theorem, has been shown to be a powerful tool for the prediction and rationalization of cluster structures and for the understanding of stereochemical nonrigidity in solution.[12,13] Although individual EHMO calculations must be regarded as much less rigorous than those of the majority of procedures listed above, a consistent interpretation for a particular species may be expected from a consideration of such properties as total (one-electron) energies, trends in one-electron energies upon geometrical rearrangement, and symmetry arguments based on Jahn-Teller theory.

In this study we examine the structures of some four- through nine- and eleven-membered homopolyatomic ions using the EHMO procedure, exploring plausible alternative geometries and possible nonrigidity in solution, according to

(1) Gillespie, R. J.; Passmore, J. *Adv. Inorg. Chem. Radiochem.* **1975**, *17*, 49 and references therein.
(2) "Homoatomic Rings, Chains and Macromolecules of Main Group Elements", Rheingold, A. L., Ed.; Elsevier: Amsterdam, 1977, and references therein.
(3) Corbett, J. D.; Rundle, R. E. *Inorg. Chem.* **1964**, *3*, 1408.
(4) Corbett, J. D. *Inorg. Chem.* **1968**, *7*, 198.
(5) Burns, R. C.; Gillespie, R. J.; Luk, W.-C. *Inorg. Chem.* **1978**, *17*, 3596.
(6) Brown, I. D.; Crump, D. B.; Gillespie, R. J.; Santry, D. P. *Chem. Commun.* **1968**, 853.
(7) Corbett, J. D. *Inorg. Nucl. Chem. Lett.* **1969**, *5*, 81.
(8) Tanaka, K.; Yamabe, T.; Terama-e, H.; Fukui, K. *Inorg. Chem.* **1979**, *18*, 3591.
(9) Rothman, J. J.; Bartell, L. S.; Ewig, C. S.; Van Wazer, J. R. *J. Comput. Chem.* **1980**, *1*, 64.
(10) Salahub, D. R.; Foti, A. E.; Smith, V. H., Jr. *J. Am. Chem. Soc.* **1978**, *100*, 7847; *Chem. Phys. Lett.* **1978**, *57*, 33.
(11) Tanaka, K.; Yamabe, T.; Terama-e, H.; Fukui, K. *Nouv. J. Chim.* **1979**, *3*, 379.
(12) Muetterties, E. L.; Hoel, E. L.; Salenture, C. G.; Hawthorne, M. F. *Inorg. Chem.* **1975**, *14*, 950.
(13) Muetterties, E. L.; Beier, B. F. *Bull. Soc. Chim. Belg.* **1975**, *84*, 397.

0020-1669/82/1321-0799$01.25/0

Table II. Observed and Calculated Bond Distances for the Polyatomic Anions and Cations

species	symmetry	obsd or calcd bond dist, Å	ref
Te_4^{2+}	D_{4h}	2.665 (×4)	20
	T_d	2.665 (×4)	
Bi_4^{2-}	D_{4h}	2.939 (×4)	21
Sn_5^{2-}	D_{3h}	2.877 (×6),[a] 3.095 (×3)[b]	22
	C_{4v}	2.950 (×8)	
	D_{5h}	2.877 (×5)	
Bi_5^{3+}	D_{3h}	3.040 (×6),[a] 3.040 (×3)[b]	5
		2.962 (×6),[a] 3.195 (×3)[b]	
		3.040 (×6),[a] 3.400 (×3)[b]	
Pb_5^{2-}	D_{3h}	3.002 (×6),[a] 3.238 (×3)[b]	22
Te_6^{4+}	D_{3h}	2.681 (×6),[c] 3.134 (×3)[d]	23
	O_h	2.832 (×12)	
	D_{6h}	2.681 (×6)	
P_6^{4-}	D_{6h}	2.149 (×6)	24
Te_6^{2+}	D_{6h}	2.750 (×6)	*k*
P_7^{3-}	C_{3v}	2.210 (×3),[a] 3.400 (×3),[b]	25
		2.170 (×3),[e] 2.250 (×3)[f]	
Sb_7^{3-}	C_{3v}	2.795 (×3),[a] 4.281 (×3),[b]	26
		2.703 (×3),[e] 2.858 (×3)[f]	
S_8^{2+}	C_s, C_{2v} (×2)[i]	2.038 (×8), 2.860 (×1),[g]	27
		2.968 (×2)[g]	
	D_{2d}, O_h	2.282 (×12)	
	D_{8h}	2.129 (×8)	
	D_{3h}	2.129 (×9), 3.217 (×6)[l]	
Sn_9^{4-}	C_{4v}	2.957 (×4),[a] 3.243 (×4)[b]	
		2.971 (×8),[e] 2.964 (×4)[f]	
	D_{3h}	3.033 (×6),[c] 3.497 (×3),[d]	
		2.896 (×12)[h]	
	C_{4v}[j]	2.957 (×4),[a] 3.243 (×4),[b]	
		2.971 (×4),[e] 2.964 (×4)[f]	
P_{11}^{3-}	D_3	2.236 (×6),[a] 2.173 (×6),[b]	
		2.236 (×3)[b]	

[a] Axial-waist distances. [b] Waist-waist distances. [c] Triangular face distances. [d] Interfacial distances. [e] Waist-base distances. [f] Base-base distances. [g] Cross-ring distances. [h] Capped face distances. [i] Exo-exo and endo-endo geometries. See text. [j] Monocapped cube structure. [k] Assumed value. [l] Taken from the S-S distance P_4S_3. See ref 2.

the above criteria. Although subject to a more exact treatment, as indicated above, some of these species have been included here for comparison since alternative geometries have not been previously investigated. When applicable, analogies to related borane and carborane structures are also noted, as well as reasons for structural differences in these systems caused by different numbers of skeletal electrons, within the framework of Jahn–Teller theory.

Calculations

All calculations were performed with the extended-Hückel approach, similar to that described by Hoffmann.[14] In the majority of cases all valence electrons were included and the basis sets were the *n*s and *n*p Slater orbitals, including orbital exponents (ξ_r) on each atom. Outer nd orbitals were assumed to play only a minor role in the bonding of the ions because of their unfavorable radial characteristics and the considerable energy differences between the *n*p and *n*d levels and so were not included in this study. Diagonal matrix elements of the Hamiltonian, H_{ii}, were either calculated from Moore's tables of atomic energy levels[15] or were taken from published values of valence-state ionization potentials (VSIP). These are listed in Table I. Because of the considerable 6s–6p separation and relatively less favorable overlap for heavier elements, calculations on polyatomic ions of the sixth row were made with only the 6p orbitals as a basis set, the 6s orbitals being regarded as filled. Off-diagonal elements of the Hamiltonian, H_{ij}, were calculated from the Wolfsberg–Helmholtz[18] and Mulliken[19] formula $H_{ij} = 0.5(H_{ii} + H_{jj})KS_{ij}$, where S_{ij} is the overlap integral. The value of K was taken as 2.00 throughout this work.

Idealized geometries (see Table II for important bond lengths) were used in all calculations, with the relevant interatomic parameters taken from reported structures. For alternative cluster geometries, a weighted average bond distance calculated from all of the reasonable bond distances in the known structure was used. However, if an example of the particular alternative geometry were known for a related ion, then the bond distances were proportioned according to this species with a weighted average bond distance equal to that of the observed structure. For alternative planar geometries involving occupied π orbitals, bond distances were assumed equal to the average of the shortest equivalent (in an idealized geometry) directly bonded distances in the observed structure. This probably furnishes a slightly overestimated bond distance because of the partial double-bond character required in these geometries but, as found for Te_4^{2+}, is not critical to the arguments presented here.

Overlap was calculated with the program POLYATOM,[30] the Slater orbitals being expressed as the sum of either six or four Gaussian-type orbitals, according to the procedure of Stewart.[31] Species containing either fourth- or sixth-row elements are not amenable to this method since a nonintegral exponent occurs in the expression for the radial function and so overlap cannot be analytically evaluated. Hence, in those calculations involving sixth-row elements, the two-center σ and π 6p–6p overlap integral expressions were first derived from the corresponding 5p–5p expressions employing the procedure of Lofthus[32] and then used to construct the respective overlap diagrams (s vs. p). The overlap diagrams for the nonintegral exponent were subsequently obtained by extended graphical interpolation. In every calculation all overlaps were included. Solution of the secular equation was carried out with an SCF program, kindly provided by Dr. D. P. Santry of this department, which was modified for extended-Hückel calculations.

Results and Discussion

The homopolyatomic cations and anions on which calculations were performed were the Te_4^{2+}, Bi_4^{2-}, Sn_5^{2-}, Bi_5^{2-}, Pb_5^{2-}, Te_6^{4+}, P_6^{4-}, Te_6^{2+}, P_7^{3-}, S_8^{2+}, Sn_9^{4-}, and P_{11}^{3-} ions. These ions were chosen as representative of the four- through nine- and eleven-atom species. The choice of a particular ion was somewhat arbitrary in cases where more than one example

(14) Hoffmann, R. *J. Chem. Phys.* **1963**, *39*, 1397.
(15) Moore, C. E. "Atomic Energy Levels: As Derived From The Analysis of Optical Spectra"; U.S. Printing Office: Washington, D.C., 1949–1958; Vols. 1–3.
(16) Bartell, L. A.; Su, L. S.; Yow, H. *Inorg. Chem.* **1970**, *9*, 1903.
(17) Greenwood, N. N.; Perkins, P. G.; Wall, D. H. *Symp. Faraday Soc.* **1967**, *1*, 51.
(18) Wolfsberg, M.; Helmholtz, L. *J. Chem. Phys.* **1952**, *20*, 837.
(19) Mulliken, R. S. *J. Chem. Phys.* **1949**, *46*, 497, 675.
(20) Couch, T. W.; Lokken, D. A.; Corbett, J. D. *Inorg. Chem.* **1972**, *11*, 357.
(21) Cisar, A.; Corbett, J. D. *Inorg. Chem.* **1977**, *16*, 2482.
(22) Edwards, P.; Corbett, J. D. *Inorg. Chem.* **1977**, *16*, 903; *J. Chem. Soc., Chem. Commun.* **1975**, 984.
(23) Burns, R. C.; Gillespie, R. J.; Luk, W.-C.; Slim, D. R. *Inorg. Chem.* **1979**, *18*, 3086; *J. Chem. Soc., Chem. Commun.* **1976**, 791.
(24) Schmettow, W.; Lipka, A.; von Schnering, H. G. *Angew. Chem., Int. Ed. Engl.* **1974**, *13*, 345.
(25) Dahlmann, W.; von Schnering, H. G. *Naturwissenschaften* **1972**, *59*, 420.
(26) Adolphson, D.; Corbett, J. D.; Merryman, D. J. *J. Am. Chem. Soc.* **1976**, *98*, 7234; **1975**, *97*, 6267.
(27) Davies, C. G.; Gillespie, R. J.; Park, J. J.; Passmore, J. *Inorg. Chem.* **1971**, *10*, 2781.
(28) Corbett, J. D.; Edwards, P. A. *J. Am. Chem. Soc.* **1977**, *99*, 3313.
(29) Wichelhaus, W.; von Schnering, H. G. *Naturwissenschaften* **1973**, *60*, 104.
(30) POLYATOM, Quantum Chemistry Program Exchange, Bloomington, Indiana.
(31) Stewart, R. F. *J. Chem. Phys.* **1970**, *52*, 431.
(32) Lofthus, A. *Mol. Phys.* **1962**, *5*, 105.

Table III. Total Energies (E_T) and the Energy Differences between the HOMO and LUMO (ΔE_{HL}) for Some Polyatomic Anions and Cations

ion	idealized structure	symmetry	E_T, eV	ΔE_{HL},[e] eV
Te_4^{2+}	square plane	D_{4h}	−297.8	2.6
	tetrahedron	T_d	−288.0	0.0
	butterfly[a]	C_{2v}	−293.0	2.8
	flattened butterfly	D_{2h}	−291.9	0.4
Sn_5^{2-}	trigonal bipyramid	D_{3h}	−284.7	4.4
	square-based pyramid	C_{4v}	−283.2	0.0
	pentagon	D_{5h}	−287.3	0.2
Te_6^{4+}	trigonal prism	D_{3h}	−432.6	1.5
	octahedron[b]	O_h	−426.4	4.0
	octahedron[c]	O_h	−426.1	4.9
	boat[d]	C_{2v}	−435.2	4.0
	flattened boat	D_{2h}	−427.7	0.3
	hexagon	D_{6h}	−434.8	0.0
S_8^{2+}	exo-endo geometry	C_s	−700.5	1.8
	endo-endo geometry	C_{2v}	−700.1	4.8
	exo-exo geometry	C_{2v}	−699.3	0.8
	octagon	D_{8h}	−699.4	1.0
	regular cuneane	D_{2d}	−692.0	0.0
	cube	O_h	−633.1	3.9
	bicapped trigonal prism	D_{3h}	−701.6	8.9
Sn_9^{4-}	monocapped square antiprism	C_{4v}	−509.8	7.3
	tricapped trigonal prism	D_{3h}	−508.2	6.8
	monocapped cube	C_{4v}	−464.9	1.5

[a] Angle between planes (or "wings") is 90°. [b] Optimized value of E_T, for which all nearest neighbors are 2.945 Å distant. See text. [c] All nearest neighbors are 2.832 Å distant—the average of all bonding distances in the observed trigonal prismatic structure. [d] Both end triangular faces in the trigonal prism have been folded back ca. 14°, for which the maximum value of E_T is obtained. See text. [e] A value of 0.0 in this column implies an open shell.

exists although heavier atom homologues were, in general, chosen, while in other cases only one example is currently known. Furthermore, this study was limited to those ions which have cluster, cage, or planar ring structures as these species are particularly amenable to this kind of calculation, which produces a considerable amount of information concerning the observed geometry. For many of the above species, plausible alternative geometries were also examined, and the relevant data required for such comparisons are listed in Table III. In this table the total energy (E_T), that is, the sum of the one-electron energies, is listed together with the energy difference (ΔE_{HL}) between the highest occupied MO (HOMO) and lowest unoccupied MO (LUMO).

Before each system is discussed individually, some general comments are relevant. For each ion, the (*observed*) geometry was always found to give a closed-shell configuration accounting for the diamagnetism of the ion. Generally, after the lowest energy orbitals were progressively filled with the appropriate number of valence electrons, there then occurred an energy gap between the HOMO and LUMO. This separation (ΔE_{HL}) varied from 1.5 eV for Te_6^{4+} to 9.4 eV for P_7^{3-}. In every case the lowest n MO's (where n is the number of atoms) always had the symmetries of the irreducible representation generated by the s orbitals in the geometry being considered. These MO's always exhibited a fairly high s character, especially for calculations involving heavy atoms, reflecting, in part, an overemphasis placed on the disparity between the s and p orbital energies in molecules or ions by use of VSIP's calculated for isolated atoms. The amount of s involvement in the bonding (in "s–p hybridization") decreases as the principal quantum number becomes larger; e.g., examination of the AO densities (as derived from a population analysis) for P_7^{3-} and Sb_7^{3-} shows that s involvement is considerably less in the Sb_7^{3-} anion. Similar trends have been noted in the series S_4^{2+}, Se_4^{2+}, and Te_4^{2+}[8] and for the S_8^{2+} and Se_8^{2+} cations.[11] As has been pointed out above, in our calculations on species containing sixth-row elements, the 6s orbitals were regarded as filled; that is, there is an "inert pair" on each atom, so that the number of bonding MO's was just sufficient to hold the total number of p valence electrons.

In almost every case, the results in Table III show the observed structure to be the most stable, albeit marginally for some ions, e.g., S_8^{2+} and Sn_9^{4-}. Other possible geometries were usually less stable or electronically unstable and subject to Jahn–Teller distortion leading to the observed geometry. When first-order Jahn–Teller (FOJT) arguments were invoked, no problems were encountered provided that the calculated MO scheme for the particular geometry gave the required orbitally degenerate state, as was generally the case. However, second-order Jahn–Teller (SOJT) arguments require criteria based not only on symmetry but also on energetic considerations and depend on the reliability of MO calculations.

If two (or more) alternative geometries have very similar total energies, then, according to SOJT theory,[33-35] the symmetries of the ground state and the first excited state (or next one or two excited states if they are close) dictate the type of nuclear displacement that will occur most easily. Thus, if the direct product of the irreducible representations of the HOMO and LUMO, when resolved into the sum of the irreducibles (designated here as Γ_{HL}), contains one of the normal vibrational modes which transforms the molecule into a new geometry, and the HOMO–LUMO energy gap is small, then the molecule will rearrange to the new geometry via this normal mode. This SOJT instability is usually considered to be possible for a HOMO–LUMO gap (ΔE_{HL}) of ca. 4 eV (310 nm), although important SOJT effects can occur for an energy gap of at least 5 eV.[33] As is common with the extended-Hückel approach with the parameterization used in this study, the calculations presented here for cluster geometries generally overestimate the value of ΔE_{HL} and imply that these ions should be colorless while, in fact, most have electric-dipole transitions in the visible region. For example, EHMO calculations gave a ΔE_{HL} for P_7^{3-} of 9.4 eV, while with the SCF–MO–CNDO procedure of Sichel and Whitehead (see below) a somewhat lower value of 7.61 eV may be obtained (also, see discussion on Sn_9^{4-}, part V, below).

For planar geometries with π manifolds, however, EHMO calculations generally give a somewhat more reliable value for ΔE_{HL} because of the ability of this procedure to mimic the results of accurate SCF calculations for the π manifold. In the case of Te_4^{2+}, for which a number of different types of calculations have been reported, ΔE_{HL} was found to be 6.86 eV from an ab initio pseudopotential SCF method, about 5.5 eV for an INDO-type calculation, and 0.92 eV with the SCF–Xα–SW procedure.[10] The first is somewhat high and the last very low. Such a dispersion of values was also reflected in the respective calculations of the $\pi(e_g) \rightarrow \pi^*(b_{1u})$ and $\pi(e_g) \rightarrow n^*(e_u)$ (or $n(e_u) \rightarrow \pi^*(b_{1u})$)[9] optical transitions for this cation. Similar results also occur for the S_4^{2+} and Se_4^{2+} cations.[8,10] In this study the EHMO procedure gave a ΔE_{HL} of 2.6 eV for Te_4^{2+}, which is intermediate between the above limits. Good agreement was also obtained with the observed absorption spectrum of Te_4^{2+}, the calculations giving energies of 2.6 and 3.1 eV for the $\pi \rightarrow \pi^*$ and $n \rightarrow \pi^*$ transitions, respectively, which are quite close to the observed values of 510 nm (2.43 eV) and 420 nm (2.95 eV).[1]

Finally, it should also be noted that unless constrained by symmetry, the calculated HOMO in many of the species dealt

(33) Pearson, R. G. *J. Am. Chem. Soc.* **1969**, *91*, 1252, 4947.
(34) Bartell, L. S. *J. Chem. Educ.* **1969**, *45*, 754.
(35) Bader, R. F. W. *Can. J. Chem.* **1962**, *40*, 1164.

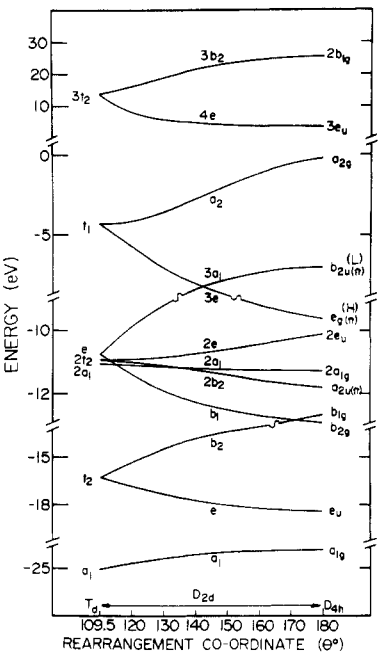

Figure 1. MO correlation diagram of Te_4^{2+} for a tetrahedron (T_d) rearranging through a symmetry-allowed motion into a square plane (D_{4h}) via a D_{2d} intermediate. The rearrangement coordinate is the angle two opposite atoms make with the centroid of the structure; H and L represent the HOMO and LUMO for Te_4^{2+}, respectively.

with here may be one of a number of very weakly bonding MO's of similar energy, several of which might be candidates to interact with the LUMO(s) and lead to SOJT rearrangement.

(I) Four-Atom Species. Four geometries were investigated for the four-atom Te_4^{2+} species; the square plane (D_{4h}), the tetrahedron (T_d), the butterfly (D_{2d}), and a "planar" butterfly (D_{2h}). Of these, the square plane was found to be the most satisfactory for the 22 valence electron Te_4^{2+} cation and is the structure that is observed in the solid state[20] and in solution at room temperature.[1,36] We note that in the observed MO scheme (Figure 1), the a_{2u}, e_g, and b_{2u} MO's form an "aromatic" π manifold with six electrons filling the a_{2u} and e_g levels, analogous to the $C_4H_4^{2-}$ anion. The tetrahedron was found to give a closed-shell configuration for a 20 valence electron system such as exhibited by the well-known P_4 and As_4 molecules. However, under T_d symmetry, a 22 valence electron system results in orbital degeneracy and FOJT instability. The MO correlation diagram between the tetrahedron and square-planar structural limits is shown in Figure 1. On distortion of the tetrahedron to a D_{2d} intermediate, the strongly antibonding t_1 level splits into the a_2 and 3e levels, the former becoming progressively more antibonding but the latter more stable as this distortion increases. At the same time the essentially nonbonding e level in T_d also splits and the derived $3a_1$ level becomes increasingly antibonding in nature. Thus, this transition can occur via a series of D_{2d} structures, and, in principle, one might not need to lower the T_d symmetry all the way to D_{4h} as a singlet ground state is obtained a little to the D_{4h} side of where the 3e and 3a levels cross at $\theta \simeq 142°$. We note, however, that starting with the D_{4h} geometry the HOMO must be e_g (it is part of the π system and is essentially nonbonding) while the LUMO must be b_{2u} (also part of the π system); thus, SOJT arguments require that the Γ_{HL} is of E_u symmetry while the B_{2u} vibrational mode is the one required to convert the square plane into a tetrahedron. Hence the D_{4h} form is predicted to be stable. Furthermore, comparison of the total energy for any of the D_{2d} geometries along the rearrangement coordinate with that of the square-planar structure shows that the latter is always greater (that is, a more negative value), and, consequently, the square-planar geometry is expected to be the most favored on the basis of these arguments.

At first sight it would not seem that the butterfly (C_{2v}) and flattened butterfly (D_{2h}) geometries, both of which offer simple valence-bond descriptions, would be important because of the strain produced by the small angles in the triangular sections of these species. Nevertheless, triangles of tellurium with similar formal oxidation states on some of the atoms have been observed in the Te_6^{4+} and $Te_3S_3^{2+}$ cations.[23,37] Calculations show, however, that neither the C_{2v} nor D_{2h} structural possibilities have as large total energies as the square-planar geometry and that only for the C_{2v} geometry is the energy gap between the HOMO and LUMO comparable to that in the observed structure. Again, resort to SOJT arguments shows that the square-planar geometry is stable with respect to any out-of-plane motion, which would give the C_{2v} structure, while the E_u vibrational mode cannot give rise to the D_{2h} structure.

Examination of the square-planar structure in a little more depth revealed that when the size of the square of tellurium atoms was varied from 2.5 to 2.7 Å, the total energy changed by only 1.4 eV—a small difference relative to those produced by changing the geometry of the ion (see Table III). One might expect, therefore, that the directly bonded distance might reflect changes in the extent of cation–anion interaction. This appears to be the case as the Te–Te distance in both $Te_4(AlCl_4)_2$ and $Te_4(Al_2Cl_7)_2$ is about 2.665 (2) Å,[20] while in $Te_4(SbF_6)_2$ it is 2.688 (3) Å.[38] Similarly, for the isovalent Se_4^{2+} cation, the Se–Se distance ranges from 2.260 (4) Å (average) in $Se_4(Sb_2F_4^{2+})(Sb_2F_5^{+})(SbF_6^{-})_5$ to 2.283 (4) Å in $Se_4(HS_2O_7)_2$.[38,39] This suggests slightly stronger cation–anion interactions, leading to longer bond lengths, in those salts with more polarizable anions or, alternatively, the one providing the highest charge density (or ionic potential) around the cation. Associated with these changes is, in this simple model, a very strong dependence of the energy of the $\pi \rightarrow \pi^*$ ($^1A_{1g} \rightarrow {}^1E_u$) transition on bond distance, which decreases in energy quite markedly as the bond length increases. Thus, for example, while $Se_4(AsF_6)_2$ and $Se_4(Sb_2F_4)(Sb_2F_5)(SbF_6)_5$ are yellow, $Se_4(HS_2O_7)_2$ is bright orange, which reflects the shift in the $\pi \rightarrow \pi^*$ transition and is in accord with the observed bond length trends for these compounds.

For the isovalent Bi_4^{2-} anion (D_{4h} geometry), ΔE_{HL} was estimated to be 4.3 eV, with an e_g HOMO and an e_u LUMO, the latter being marginally more stable (ca. 0.1 eV) than the b_{2u} level, the LUMO for the Te_4^{2+} cation. This is probably an artifact of the calculation because of the exclusion of the 6s orbitals from the basis set, incorporation of which would destabilize the e_u level. The relatively large ΔE_{HL} and lack of an alternative geometry (T_d is FOJT unstable) for an intramolecular rearrangement pathway therefore indicates that Bi_4^{2-}, like Te_4^{2+}, would retain its square-planar structure in solution.

(II) Five-Atom Species. Three geometries were examined for the Sn_5^{2-} anion, the trigonal bipyramid (D_{3h}), the square-based pyramid (C_{4v}), and the regular pentagon (D_{5h}). All three had similar total energies with the pentagon nominally the most stable. This is probably the result of the assumed bond lengths. Of these three structures, only the D_{3h} geometry was found to give an acceptable closed-shell MO

(36) Schrobilgen, G. J.; Burns, R. C.; Granger, P. *J. Chem. Soc., Chem. Commun.* **1978**, 957.

(37) Gillespie, R. J.; Luk, W.-C.; Maharajh, E.; Slim, D. R. *Inorg. Chem.* **1977**, *16*, 892.

(38) Gillespie, R. J.; Sawyer, J. F.; Vekris, J. E., unpublished results.

(39) Brown, I. D.; Crump, D. B.; Gillespie, R. J. *Inorg. Chem.* **1971**, *10*, 2319.

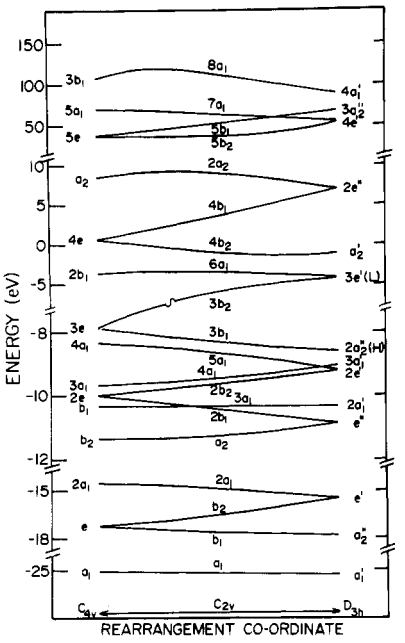

Figure 2. MO correlation diagram of Sn_5^{2-} for a square-based pyramid (C_{4v}) rearranging through a symmetry-allowed motion into a trigonal bipyramid (D_{3h}) via a C_{2v} intermediate; H and L represent the HOMO and LUMO for Sn_5^{2-}, respectively.

configuration for a 22 electron count (see Figure 2), and this is the observed structure for the Sn_5^{2-} and Pb_5^{2-} anions in the solid state.[22] Furthermore, a recent vibrational spectroscopic study of the isovalent Bi_5^{3+} cation showed that this cation also has a D_{3h} geometry and that this structure is maintained in the solid state and in solution.[5] The, as yet unsynthesized, *closo*-$B_5H_5^{2-}$ anion, which would have the same skeletal electron count, is likewise predicted to adopt a D_{3h} geometry,[40] and such a prediction is strengthened by the observed trigonal-bipyramidal structures of the neutral carborane analogues 1,2- and 1,5-$C_2B_3H_5$.[41]

As is clear from Figure 2, which shows the MO correlation diagram between the C_{4v} and D_{3h} structural limits, the square-pyramidal (C_{4v}) geometry gives a closed-shell configuration for 20 or 24 valence electrons, while with 22 valence electrons an open shell is obtained. The resulting instability (there would be a low-lying triplet state) and subsequent distortion would lead, via a C_{2v} intermediate, to the more stable D_{3h} rearrangement.

The third geometry, the regular pentagon (D_{5h}), has a total energy slightly greater than that for the trigonal bipyramid and also gives a closed-shell configuration. However, examination of the eigenvector matrix showed that, although there were the correct number of strongly bonding orbitals and that the π manifold was accounted for—filled a_2'' and e_1'' bonding orbitals and a vacant e_2'' orbital—for an acceptable MO scheme the formally weakly bonding LUMO (which is not part of the π system) would have to be filled. Furthermore, with 22 valence electrons the calculated MO configuration for the pentagon is unstable in the second order as Γ is $E_1'' \times E_1'' = A_1'' + A_2'' + E_2''$, in this case relating the second highest occupied MO and the LUMO, with an energy gap of 0.8 eV between these levels. Thus Γ contains an E_2'' irreducible which is the symmetry of the required out-of-plane motion that gives rise to observed trigonal-bipyramidal geometry.

The isovalent Bi_5^{3+} and Pb_5^{2-} species each exhibited closed-shell configurations for D_{3h} geometries and had fairly

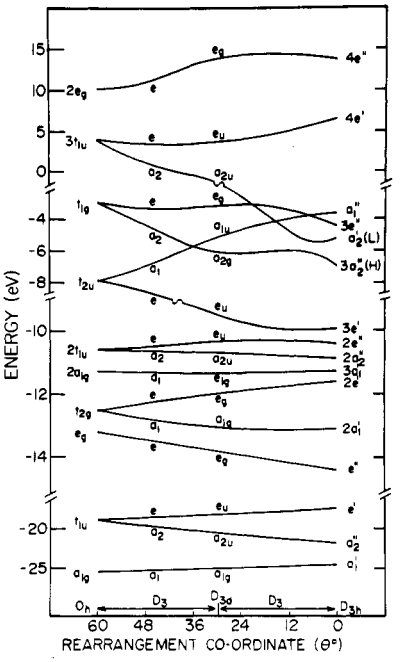

Figure 3. MO correlation diagram of Te_6^{4+} for an octahedron (O_h) rearranging through a symmetry-allowed motion into a trigonal prism (D_{3h}) via D_3 and D_{3d} intermediates. The rearrangement coordinate is the angle between the two triangular planes around the unique C_3 axis; H and L represent the HOMO and LUMO for Te_6^{4+}, respectively.

large ΔE_{HL}'s with a range of 4.0–4.7 eV for the three Bi_5^{3+} geometries (of different dimensions; see ref 5) and 5.8 eV for the Pb_5^{2-} anion. In all cases the HOMO and LUMO were of e'' and e' symmetry, respectively. With the large ΔE_{HL} values for these species especially Pb_5^{2-}, and as the C_{4v} geometry gives an open shell (viz., Sn_5^{2-}), there is no viable low-energy pathway for internuclear rearrangement so that the D_{3h} structures would be expected to be stable in solution. Indeed, the trigonal-bipyramidal geometry for Bi_5^{3+} has previously been identified in solution in molten $NaAlCl_4$ at 180 °C.[5]

(III) Six-Atom Species. For six-atom systems, two different valence-electron counts have been found, and a variety of structural forms have been characterized. The Te_6^{4+} cation has 32 valence electrons and represents the only known example of an isolated trigonal-prismatic (D_{3h}) cluster.[23] In contrast, for a 34 valence electron count, the heteroatomic $Te_3S_3^{2+}$ and $Te_2Se_4^{2+}$ cations[37] each have a boat-shaped six-membered ring with a cross-ring bond (C_s), while the homoatomic P_6^{4-} anion, which is the formal anionic unit assumed to be present in the alkali-metal phosphides Rb_4P_6 and K_4P_6,[24] has a planar six-membered ring (D_{6h}).

The six-atom 32 valence electron Te_6^{4+} cation was extensively investigated in this study. Alternative geometries that were investigated were the trigonal prism (D_{3h}), octahedron (O_h), a trigonal prism which was progressively opened along one of the edges connecting the triangular faces, i.e., to give a boat (C_{2v}), ultimately leading to a planar structure (D_{2h}), and a regular hexagon (D_{6h}).

The trigonal-prismatic geometry gave a closed shell for 32 valence electrons (Figure 3), in accord with the structure of Te_6^{4+} observed in the solid state and in solution.[23,36] The octahedron (or trigonal antiprism) also gave a closed shell for 32 valence electrons. However, the total stabilization energy of the octahedral arrangement is considerably less (by 6.5 eV) than the trigonal prism when the averaged Te–Te distance (2.832 Å) is used for the sides of the octahedron and is only marginally improved when the total energy is "minimized" by varying the dimensions of the octahedron (E_T gives an

(40) Moore, E. B., Jr.; Mohr, L. L., Jr.; Lipscomb, W. N. *J. Chem. Phys.* **1961**, *35*, 1329.
(41) Ditter, J. F. *Inorg. Chem.* **1968**, *7*, 1748 and references therein.

energy minimum for Te–Te = 2.945 Å). The less favorable stability in the case of the O_h geometry is a consequence of the appreciable antibonding nature of the filled t_{2u} orbital, the HOMO in this system. The MO correlation diagram between the D_{3h} and O_h limits (see Figure 3) is fairly straightforward except that in the D_3 intermediate the $3a_2$ and $4a_2$ levels, which derive respectively from the t_{1g} and $3t_{1u}$ MO's in O_h, closely approach each other, avoid crossing (the "noncrossing rule" for exact or approximate electronic states), and result in the $3a_2''$ and a_2' MO's, respectively—the HOMO and LUMO in the D_{3h} geometry. The close approach of these levels, combined with the changes in energy of the $3a_2$ level (the HOMO in the D_3 intermediate for $\theta < 38°$) along the rearrangement coordinate, gives rise to a secondary minimum in total energy between the D_{3h} and O_h structural limits. This occurs when the angle along the rearrangement coordinate (i.e., rotation about a C_3) axis) is ca. 17° from the D_{3h} limit; this minimum, however, is still ca. 0.9 eV less stable than that of the latter limit. It should be noted that in the structure of the Te_6^{4+} cation in $Te_6(AsF_6)_4 \cdot 2AsF_4$ the two triangular faces are rotated by 2.7° relative to each other. A similar twist is not observed in $Te_6(AsF_6)_4 \cdot 2SO_2$, and in the former adduct this twist is probably caused by packing effects rather than by an effect that could be attributed to the secondary minimum in energy.

For the octahedron, SOJT arguments reveal that the Γ_{HL} is $T_{2u} \times T_{1g} = A_{2u} + E_u + T_{1u} + T_{2u}$ and, since the HOMO–LUMO energy gap is only 4.0 eV, the three components of the T_{2u} vibrational mode provide the necessary trigonal twist that converts the octahedron into the more stable trigonal prism. Interestingly, for the trigonal prism Γ_{HL} is $A_2 \times A_2 = A_1$ (see also ref 42), and, as a vibrational mode of this symmetry exists and ΔE_{HL} is only 1.5 eV, the trigonal prism might be expected to convert into the octahedron. However, as established above, the trigonal prism is substantially more stable than the octahedron from EHMO calculations and, indeed, the solid-state geometry of Te_6^{4+} is trigonal prismatic, and this is maintained in solution at both −70 °C and room temperature as shown by Raman and ^{125}Te NMR studies.[36,43] While we conclude that the trigonal prism is more stable than an octahedron, more rigorous calculations might indicate that these two geometries are somewhat closer in total energy so that stereochemical nonrigidity in solution may occur at higher temperatures.

Comparison with the related borane system here is illuminating. The Te_6^{4+} cation is assigned 20 skeletal electrons and is therefore analogous to a *hypho*-borane and consequently more electron rich than *closo*-$B_6H_6^{2-}$, which has only 14 skeletal electrons. This latter borane has an octahedral geometry so that the t_{2u} LUMO in this anion would become the HOMO in octahedral Te_6^{4+} as indicated above. For the borane the octahedral geometry is actually 2.6 eV more stable than the trigonal prism and, furthermore, the HOMO–LUMO gap is greater, 6.6 eV (O_h) compared to 1.1 eV (D_{3h}).[13] Here, SOJT arguments predict a destabilization of trigonal prismatic $B_6H_6^{2-}$ relative to the octahedral structure,[13] the observed geometry.

Although the trigonal prism has been shown to be a more stable arrangement for Te_6^{4+} than an octahedron, calculations of the type presented here indicate that symmetrically

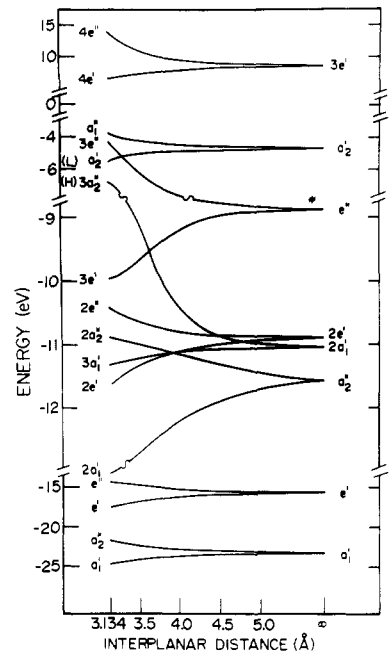

Figure 4. MO correlation diagram for the approach of two eclipsed "Te_3^{2+}" units to give a Te_6^{4+} cation. The asterisk (*) implies an unfilled orbital for "Te_3^{2+}"; H and L represent the HOMO and LUMO for Te_6^{4+}, respectively.

lengthening the trigonal prism along one of the edges, to give a boat-shaped structure with C_{2v} symmetry, gives a minimum in energy which is actually lower than the total energy for the trigonal prism. This occurs when the triangular faces have each folded back ca. 14° from their original, parallel positions. This structure also corresponds to a single valence-bond structure. Continuation of this procedure ultimately leads to a planar structure, or flattened boat (D_{2h}), but this is considerably less stable than the trigonal prism and actually only a little more stable than the octahedron. Alternatively, if the triangular faces are folded in, the energy decreases only very slightly, at least for small distortions (ca. 5°) away from the regular structure. The occurrence of the energy minimum for the opened prism may be simply an artifact of the calculation, and a closer examination of the potential surface using more sophisticated calculations with some measure of interelectron interaction would probably reveal that the trigonal prism actually represents the minimum on this surface.

The Te_6^{4+} cation can also be thought of as arising from the interaction of two eclipsed Te_3^{2+} units. Interaction of two staggered units would give an octahedron but, as this geometry is energetically less favorable than the trigonal prism, this process was not investigated. The "Te_3^{2+}" cation would have an open shell for 16 valence electrons $[(a_1')^2(e')^4(a_2'')^2(2a_1')^2(2e')^4(e'')^2]$, and distortion to lower symmetry (e.g., C_{2v}) would be required to split the e'' level; alternatively, two Te_3^{2+} cations can interact to give the Te_6^{4+} cation. It is noted that E_T for Te_3^{2+} (D_{3h}) is −215.5 eV, so that $2E_T(Te_3^{2+})$ is less than $E_T(Te_6^{4+})$, and some stabilization (1.6 eV) is gained on formation of the Te_6^{4+} "dimer".[44] The energy level diagram for the approach of two eclipsed Te_3^{2+} units is shown in Figure 4 and is similar, in many respects, to that reported by Evans[45] for the approach of two B_3H_3 triangles although the primarily B–H bonding orbitals were not considered in this treatment.

(42) From the results of the calculations published by Salahub et al. (ref 10, p 7855), it may be shown that for a hypothetical S_6^{4+} ($\approx S_6^{6+}$) with S–S distances of 2.06 Å (triangular face) and 2.40 Å (long bond, rectangular face)—the same relative dimensions as found for Te_6^{2+}—the HOMO and LUMO are of a_2'' and a_2' symmetry, respectively, and are identical with that in Te_6^{4+}. As ΔE_{HL} is also only ca. 1.4 eV, then, even if this value has been slightly underestimated as is common with the SCF–Xα–SW method, it is apparent that S_6^{4+} is amenable to the same type of SOJT considerations as described for the Te_6^{4+} cation.

(43) Burns, R. C.; Gillespie, R. J., in preparation.

(44) For a 16 valence electron triatomic system, the stable geometry is predicted to be linear by Walsh's arguments (*J. Chem. Soc.* **1953**, 2266). For such a geometry, $E_T(Te_3^{2+})$ is −217.4 eV so that $2E_T(Te_3^{2+})$ is now greater than $E_T(Te_6^{4+})$. However, it should be noted that $E_T(Te_6^{4+})$ was not minimized in this study and only the observed geometry was used to calculate $E_T(Te_6^{4+})$.

(45) Evans, J. *J. Chem. Soc., Dalton Trans.* **1978**, 18.

At a distance of about 5 Å, the orbitals form symmetric and antisymmetric combinations, with considerable orbital mixing on closer approach. In particular, strong interactions occur for the π out-of-plane orbitals, a_2'' and e'', as well as the $2a_1'$ level. Examination of the fate of the half-filled e'' levels in the Te_3^{2+} units, which constitute the upper part of the π manifold in each system, shows that they interact to give the $3e'$ and $3e''$ levels. The former is slightly stabilized while the latter combination is highly destabilized. In the trigonal prism only the $3e'$ level is filled (the $3e''$ is antibonding) and this accounts for the stability of the trigonal prism. Interaction of the lower parts of the π manifold on each Te_3^{2+} unit, a_2'', gives the filled (bonding) $2a_1'$ and filled (antibonding between the planes but bonding within the triangles) $2a_2''$ orbitals, while in the trigonal prism the $3a_2''$ HOMO (antibonding between the planes and essentially nonbonding within the triangles) derives from the $2a_1'$ levels on the isolated triangles.[46] Roughly speaking, there are two bonds between the two triangular rings which are symmetrically arranged about the structure, and these may be pictorially represented by three resonance forms in a valence-bond description of the cation (see ref 23).

The final structure that was examined for Te_6^{4+} was a regular hexagon (D_{6h}). Although slightly more stable than the trigonal prism, an open shell was obtained with a half-filled e_{2u} level, suggesting that a less oxidized species such as Te_6^{2+} (with 34 valence electrons) might adopt this geometry. Indeed, the isovalent P_6^{4-} has been found to have such a structure. For P_6^{4-} and Te_6^{2+} closed-shell configurations were obtained with HOMO–LUMO energy gaps of 4.1 and 1.8 eV, respectively. In both cases an "aromatic" π manifold was obtained (a_{2u}, e_{1g}, e_{2u}, and b_{2g}), the three lowest levels being filled to give a 10 π-electron Hückel system. Furthermore, Γ_{HL} for both ions is $E_{2u} \times B_{2g} = E_{1u}$, and, as the E_{1u} vibrational mode is an in-plane distortion, these systems should be stable to any out-of-plane rearrangement of structure (the trigonal prism is energetically unfavorable, while the octahedron gives an open shell). It is suggested, therefore, that the structurally uncharacterized Te_6^{2+} cation has an hexagonal geometry. In passing, it is noted that $Te_6(AlCl_4)_2$ has been reported to have an hexagonal unit cell,[47] which lends some support to the above conclusion, while a recent[48] ^{125}Te Mössbauer study of $Te_6(AlCl_4)_2$ provided no evidence for more than one tellurium site in the compound, as expected for the planar structure but not for a boat structure similar to that of the $Te_3S_3^{2+}$ and $Te_2Se_4^{2+}$ cations.[37] Neither of these heteroatomic species has a D_{6h} π manifold (their symmetries are both C_s), and they are more stable with the cationic charge localized on the less electronegative tellurium atoms, which form the bridgehead (three coordinate) positions in these nonplanar species.

(IV) Eight-Atom Species. The S_8^{2+} cation has a rather unusual structure with an exo–endo conformation of atoms (C_s) and a cross-ring bond.[27] In contrast, *cyclo*-octasulfur, S_8, has the well-known crown or exo–exo conformation (D_{4d}) and no cross-ring bond.[49] For S_8^{2+}, seven geometries were investigated: the observed exo–endo geometry (C_s), and endo–endo arrangement of atoms where the "exo-sulfur" atom is the observed S_8^{2+} structure is flipped up into an "endo-position" opposite that of the original "endo-sulfur" atom (C_{2v}), the corresponding exo–exo structure (C_{2v}), a cuneane structure with all nearest neighbor distances equal (D_{2d}), a bicapped trigonal prism (D_{3h}), a cube (O_h), and a planar octagon structure (D_{8h}).

Initially, the S_8^{2+} species may be considered in terms of the octagon. This geometry was found to be slightly less stable than the observed structure and, moreover, with 14 electrons in the π manifold (a_{2u}, e_{1g}, e_{2u}, e_{3g}, and b_{2u}) has only marginal π stabilization. The π bonding may be avoided by localizing electrons in lone pairs and σ bonding, as in the exo–exo, exo–endo, and endo–endo geometries. In fact, these geometries may easily be derived from the octagon by out-of-plane displacements of the relevant atoms and by formation of a cross-ring bond in each case. All three of these geometries have very similar total energies, with the observed exo–endo structure nominally the most stable. However, as ΔE_{HL} favors the endo–endo geometry, one might have expected S_8^{2+} to adopt this conformation as a large HOMO–LUMO gap is one criterion for a Jahn–Teller stable structure.

Of the remaining cluster-type geometries, both the cuneane structure and the cube were found to be considerably less stable than the observed structure, while the former also has an open shell for 46 valence electrons with a half-filled 6e level. The bicapped trigonal prism, in which the three-coordinate sulfur atoms cap the prism, gives an enticing valence-bond structure and was also marginally more stable than the observed structure. However, objections can be raised against this geometry due to some destabilization induced by the π-type interactions of the eclipsed lone pairs, for which calculations of this type do not take account.

Comparison of our data with that of Salahub et al.,[10] the latter calculated with the SCF–Xα–SW procedure, reveal many similarities. In both studies the D_{2d} geometry as exhibited by S_4N_4 gives an open shell for 46 valence electrons. It should be noted that slight distortion of this geometry, with reduction to C_{2v} symmetry, produces the endo–endo type geometry that was also investigated in our study. This actually results in a somewhat greater total energy as well as splitting of the 6e level. The SCF–Xα–Sw method showed that both the exo–endo and exo–exo geometries have closed-shell configurations with ΔE_{HL}'s of 0.62 and ca. 0.7 eV, respectively, comparable to our values of 1.8 and 0.8 eV. Also, it was concluded that on going from an exo–endo to an exo–exo conformation by flipping one end of the cation only minor effects result and that it is only on reduction of S_8^{2+} to S_8 or oxidation of S_8 to S_8^{2+} that the loss or formation of the cross-ring bond is important. Similar conclusions can be drawn from this study with regard to the conformation of S_8^{2+}, as it is apparent that there is little to indicate which of the exo–endo, exo–exo, and, in our case, endo–endo as well geometries would be the most favorable conformation for this cation.

Although no data are available on S_8^{2+} itself, a recent ^{77}Se NMR study on the related Se_8^{2+} cation, which has a structure similar to that of S_8^{2+}, shows that this cation has no tendency toward structural rearrangement that is fast on the NMR time scale.[50] It would appear, therefore, that the exo–endo structure is undoubtedly the preferred geometry and that a more exhaustive analysis of the potential surface between the exo–exo and endo–endo structural limits would be required to pinpoint the potential minimum and reasons behind the preferred structure in this case.

(V) Nine-Atom Species. The final system in which alternative geometries were investigated was the Sn_9^{4-} species, where the observed monocapped square antiprism (C_{4v}), tricapped trigonal prism (D_{3h}), and monocapped cube (C_{4v})

(46) The correlation diagram given by Salahub et al.[10] for the progressive separation of the two S_3 triangular units in trigonal prismatic S_6^{6+} covers part of the same range of interaction as given for the "Te_3^{2+}" units in Figure 4, after there was proportioning for differences in length between S–S and Te–Te bonds. Where this overlap occurs, comparison of the diagrams with regard to orbital ordering and crossing shows excellent agreement and provides considerable support for the overall validity and trends in the MO energy levels obtained in this study.

(47) Prince, D. J.; Corbett, J. D.; Garbisch, B. *Inorg. Chem.* **1970**, *9*, 2731.
(48) Jones, C. H. W. *Can. J. Chem.* **1977**, *55*, 3076.
(49) Caron, A.; Donahue, J. *Acta Crystallogr.* **1965**, *18*, 562.
(50) Burns, R. C.; Gillespie, R. J.; Schrobilgen, G. J., in preparation.

geometries were compared. All three gave a closed shell for 40 valence electrons, but the monocapped square antiprism and the tricapped trigonal prism were by far the most stable. The total energies for the latter two geometries were almost identical, and this, together with the ease of interconversion of the geometries,[28] raises the possibility of different geometries in the solid state and nonrigidity in solution. A recent ^{119}Sn NMR study on Sn_9^{4-} has shown, in fact, that this anion does undergo (*intramolecular*) exchange at 30 °C in ethylenediamine and at −40 °C in liquid ammonia.[51]

On the basis of EHMO calculations, ΔE_{HL} was found to be ca. 7 eV for both geometries, implying that SOJT effects, and subsequent interconversion of the geometries, could not occur. As the Sn_9^{4-} anion exhibits electronic transitions in the visible region, it is evident that ΔE_{HL} has been considerably overestimated in these calculations. The results of some SCF–MO–CNDO-type calculations substantiate this, giving HOMO–LUMO energy gaps (C_{4v}, 4.03; D_{3h}, 3.79 eV) ca. 45% lower than those calculated by the EHMO method. In this context SOJT arguments suggest that interconversion of the two geometries can occur.

The vibrational mode required to convert the D_{3h} geometry into C_{4v} is of E′ symmetry, while the reverse operation occurs primarily through an extended B_1 vibration. In the EHMO calculations these symmetry species may be generated from the terms relating the third-highest occupied MO ($3a_2''$) and the LUMO ($3e''$) ($A_2'' \times E'' = E'$) in D_{3h} and the third-highest occupied MO (5e) and the LUMO (6e) ($E \times E = A_1 + A_2 + B_1 + B_2$) in the C_{4v} geometry. The energy gaps are 7.3 and 8.0 eV, respectively, both only slightly greater than the ΔE_{HL} values but, as indicated above, are greatly exaggerated in the present calculations. The corresponding values calculated by the SCF–MO–CNDO-type procedure are 3.93 and 4.03 eV, respectively, and because of the different ordering of MO's, now relate the HOMO ($3a_2''$) and second-lowest unoccupied MO ($3e''$) in D_{3h} and the HOMO (5e) and LUMO (6e) in the C_{4v} geometry. These two geometries are therefore readily interconvertable. Furthermore, through the agency of these normal vibrations, all atoms can be interchanged so that, when viewed in this context, the fluxional nature of Sn_9^{4-} and equivalence of all atoms in solution is understandable. A similar rearrangement process might also be used to account for the observed nonrigidity of ReH_9^{2-} and related species in solution.[52,53]

The monocapped square antiprismatic structure for Sn_9^{4-} may be compared with that of the isovalent Bi_9^{5+} cation, which exists in the alternative D_{3h} form in $Bi^+Bi_9^{5+}(HfCl_6^{2-})_3$[54] and in an intermediate C_{2v} form in $(Bi_9^{5+})_2(BiCl_5^{2-})_4(Bi_2Cl_8^{2-})$.[55] The differences in structure exhibited by these isovalent species suggest a very subtle interplay of environment, size of atom, and internuclear repulsions and cationic or anionic nature of the species; some discussion of this is given below. The tricapped trigonal prismatic structure is also adopted by the nine-atom closo-borane anion, $B_9H_9^{2-}$.[56] Here, however, there are only 20 skeletal electrons compared to the 22 in the Sn_9^{4-} and Bi_9^{5+} ions. Also, an EHMO treatment for $B_9H_9^{2-}$ indicated that the C_{4v} geometry would require two electrons in a degenerate orbital while the D_{3h} geometry gave a closed-shell configuration for 40 valence electrons.[56] There is, accordingly, no easy rearrangement pathway for this borane, and this is reflected in its observed rigidity in solution.[12] We note in passing that the recently prepared Ge_9^{2-} anion,[57] which is isovalent with the $B_9H_9^{2-}$ anion, has an intermediate C_{2v} geometry but is derivable from the D_{3h} structural limit.[58]

Comparison of the tricapped trigonal prismatic structures of the Bi_9^{5+}, $B_9H_9^{2-}$, and Ge_9^{2-} ions reveals one significant structural difference, in that the ratio of the height of the prism to the basal edge distance is greater for Bi_9^{5+} (1.15) than for $B_9H_9^{2-}$ (0.97) or Ge_9^{2-} (1.02). Interestingly, for actual trigonal prismatic species themselves, a similar effect may be observed, with the corresponding ratio for Te_6^{4+} (1.17) greater than that found in the valence-precise prismane derivative, hexamethyl prismane (1.01).[59] Moreover, the respective ratios for the two types of prism are almost identical in both the nine- and six-atom clusters. It should also be noted that, just as Bi_9^{5+} has two more skeletal electrons than either $B_9H_9^{2-}$ or Ge_9^{2-} (22 vs. 20), Te_6^{4+} has two more skeletal electrons than hexamethyl prismane (20 vs. 18). As indicated previously for Te_6^{4+}, and also for Bi_9^{5+}, the respective HOMO's for these species, $3a_2''$ and $2a_2''$ are singly degenerate and are extensively antibonding between the triangular faces of the prism atoms in each geometry. It would appear plausible, therefore, that retention of the prismatic structure, with its subsequent elongation, in both Bi_9^{5+} and Te_6^{4+} might be attributed to similar factors. One factor that readily springs to mind is the overall charge on both cations, which places a high cationic charge on the prism atoms in Bi_9^{5+} (+0.611, compared to +0.448 for the waist atoms[3]) and on those in Te_6^{4+} (+0.667). Indeed, Bi_9^{5+} and Te_6^{4+} are, together with Bi_5^{3+}, the most highly oxidized polyatomic cations that have yet been characterized. Two consequences of the high cationic charge in these clusters are contraction of the valence orbitals; that is, they become less diffuse, leading to poorer overlap and increased internuclear repulsions. If the latter dominate energy considerations, then Coulomb law repulsion will dictate that, at least for Bi_9^{5+}, the tricapped trigonal prismatic geometry will prevail as this geometry has been shown to be more stable than the monocapped square antiprism with regard to rearrangements of points on the surface of a sphere repelling each other by Coulomb's law.[60] For Te_6^{4+} the alternative octahedral geometry has been shown above to be considerably less stable than the trigonal prism, unlike the nine-atom species where the D_{3h} and C_{4v} structural limits are very similar in energy, so that the trigonal prism would always be expected to be the observed geometry. The presence of an extra skeletal electron pair in both Bi_9^{5+} and Te_6^{4+}, with elongation of the prism in each case, may therefore be required to maintain the stability of the prismatic structure of both ions and certainly relative to the hypothetical 20 and 18 valence electron species "Bi_9^{7+}" and "Te_6^{6+}" (analogous to $B_9H_9^{2-}$ and Ge_9^{2-} and hexamethyl prismane, respectively); however, it is less obvious why the Bi_9^{5+} cation does not adopt the C_{4v} structure. Nevertheless, if internuclear repulsions are important, as suggested above, the D_{3h} geometry

(51) Rudolph, R. W.; Wilson, W. L.; Parker, F.; Craig Taylor, R.; Young, D. C.; *J. Am. Chem. Soc.* **1978**, *100*, 4629.
(52) Cotton, F. A.; Wilkinson, G. "Advanced Inorganic Chemistry", 4th ed.; Interscience: New York, 1980; p 55.
(53) The Ge_9^{4-} anion (isovalent with Sn_9^{4-}) is amenable to a similar treatment to that described for Sn_9^{4-}, having filled and vacant orbitals of required symmetry for both the C_{4v} and D_{3h} geometries. However, the calculated energy gaps are 5.97 (C_{4v}; e → e) and 5.47 (D_{3h}; $a_2'' \rightarrow e''$) eV, while in fact Ge_9^{4-} has electronic transitions in the visible region, suggesting that even in these calculations energy differences have been somewhat overestimated.
(54) Friedman, R. M.; Corbett, J. D. *Inorg. Chem.* **1973**, *12*, 1134.
(55) Hershaft, A.; Corbett, J. D. *Inorg. Chem.* **1963**, *2*, 979.
(56) Guggenberger, L. *Inorg. Chem.* **1968**, *7*, 2260.
(57) Belin, C. H. E.; Corbett, J. D.; Cisar, A. *J. Am. Chem. Soc.* **1977**, *99*, 7163.
(58) The Ge_9^{2-} anion gives a closed shell for an ideal D_{3h} geometry with an energy gap ($a_2'' \rightarrow e''$) of 6.64 eV, slightly greater than that for Ge_9^{4-}. The magnitude of this value, although probably overestimated (see ref 53), together with the fact that no satisfactory iteration results for a C_{4v} geometry, indicates that the latter geometry does not provide a low-energy pathway for rearrangement of the anion. A possible C_{2v} intermediate, however, may; see: Guggenberger, L. J.; Muetterties, E. L. *J. Am. Chem. Soc.* **1976**, *98*, 7221.
(59) Karl, B. R., Jr.; Wang, Y. C.; Bauer, S. H. *J. Mol. Struct.* **1975**, *25*, 17.
(60) Melnyk, T. W.; Knop, O.; Smith, W. R. *Can. J. Chem.* **1977**, *55*, 1745.

Table IV. Charge Distribution in Polyatomic Cations and Anions

ion	symmetry	charge distribution/atom
Te_4^{2+}	D_{4h}	+0.500[a]
Bi_4^{2-}	D_{4h}	−0.500[a]
Sn_5^{2-}	D_{3h}	axial −0.493,[d] waist −0.338[b]
Pb_5^{2-}	D_{3h}	axial −0.398,[d] waist −0.401[b]
Te_6^{4+}	D_{3h}	+0.667[a]
P_6^{4-}	D_{6h}	−0.667[a]
P_7^{3-}, Sb_7^{3-}[c]	C_{3v}	apical +0.064,[d] waist −0.963, basal −0.058
S_8^{2+}	C_s	bridgehead +0.662, "exo-S" +0.037, "endo-S" +0.028, "exo"-adjacent S +0.127, "endo-adjacent" S +0.179
Sn_9^{4-}	C_{4v}	apical −0.581, waist −0.259, basal −0.596[b]
P_{11}^{3-}	D_3	axial −0.226,[d] waist (3-coordinate) +0.257, waist (2-coordinate) −1.363

[a] All atoms symmetry equivalent. [b] Ions for which several resonance structures are required to represent the structure, implying delocalization of charge. [c] The charge distribution of Sb_7^{3-} is similar to that of P_7^{3-}. [d] Atoms on the 3-fold rotation axis.

will be favored, and, in this context, it is noted that small variations in the ratio of the height of the prism to the basal edge distance in a hypothetical D_{3h} model for Sn_9^{4-} (also a 22 skeletal electron system) show only very slight changes in the total atomization energy,[28,57] while EHMO calculations for Te_6^{4+} show that, on increasing the relative height of the prism, the total energy actually indicates a marginal increase in stabilization for this species.

Calculations on Other Species. For P_7^{3-} and Sb_7^{3-} (C_{3v}) and P_{11}^{3-} (D_3), reasonable MO schemes were obtained with closed shells, but with a large HOMO–LUMO energy gap in each case, viz., 9.4, 7.4, and 6.8 eV, respectively. This suggests that these are colorless ions, whereas in fact all have electric-dipole transitions in the visible region. Thus, like the Sn_9^{4-} anion and, indeed, most of the other species dealt with in this paper, the energy gap between the HOMO and LUMO is not reliably calculated by the extended-Hückel procedure. This inability to calculate accurate energy levels is one of the well-known deficiencies of this method as applied to systems of the type examined here, although the parameterization of the procedure has provided a realistic rationale of geometry and reactivity for boranes, carboranes, and conjugated organic systems, for which is was originally devised. For the three anions listed above, however, it may be noted that the rather large ΔE_{HL} values, although somewhat overestimated (SCF–MO–CNDO calculations do suggest about a 20% overestimation for the seven-atom species), indicate that these anions probably should not undergo rearrangement in solution.

Charge Considerations in Homopolyatomic Cations and Anions. One final consideration of the calculations reported in this work concerns the charge distribution in each ion. These data are reported in Table IV. In those systems which have symmetry equivalent atoms, all carried the same charge, as expected, while for those ions which cannot be represented by a single valence-bond structure; e.g., in Sn_9^{4-}, the formal cluster charge was fairly much delocalized over the entire system. In Sn_9^{4-}, for example, the spread of charge was similar to that obtained for this anion by the SCF–MO–CNDO calculation discussed above.[28] For those ions which can be represented by localized two-center bonding descriptions, e.g., Sb_7^{3-} and P_{11}^{3-}, the charge distributions reflected the respective conventional valence-bond structures, although for P_7^{3-} alternative SCF–MO–CNDO calculations suggest a somewhat more delocalized and realistic charge distribution.[26] Use of a self-consistent charge iteration procedure in our calculations would also decrease the disparity between the charges on the atoms. Also of considerable interest in this respect is the S_8^{2+} cation for which a single valence-bond structure can also be drawn. Here, however, the calculated charge distribution indicates that there is significant delocalization of charge to the atoms adjacent to the bridgehead sulfur positions, and this is in agreement with the results of the more nearly exact calculations recently reported for this cation.[11]

Acknowledgment. We thank Professor J. D. Corbett for kindly supplying us with the results of some semiempirical SCF–MO–CNDO-type calculations[61] on the P_7^{3-}, Sb_7^{3-}, Sn_9^{4-}, Ge_9^{4-}, and Ge_9^{2-} anions, Professor H. B. Thompson (University of Toledo) for useful comments, and the Natural Sciences and Engineering Research Council of Canada for financial support.

Registry No. Te_4^{2+}, 12597-50-1; Sn_5^{2-}, 61583-40-2; Te_6^{4+}, 62046-42-8; S_8^{2+}, 11062-34-3; Sn_9^{4-}, 12597-40-9; Bi_4^{2-}, 63951-87-1; Pb_5^{2-}, 58798-64-4; P_6^{4-}, 79933-19-0; P_7^{3-}, 39040-22-7; Sb_7^{3-}, 57348-81-9; P_{11}^{3-}, 39343-88-9; Bi_5^{3+}, 12595-67-4; Te_6^{2+}, 39448-81-2.

(61) Sichel, J. M.; Whitehead, M. A. *Theor. Chim. Acta* **1968**, *11*, 220, 239.